DISTRIBUTED PARAMETER MODELING AND THERMAL ANALYSIS OF A SPIRAL WATER WALL IN A SUPERCRITICAL BOILER

by

Shu ZHENG, Zixue LUO*, and Huaichun ZHOU

The State Key Laboratory of Coal Combustion, Huazhong University of Science and Technology, Wuhan, China

Original scientific paper
DOI: 10.2298/TSCI1305337Z

In this paper, a distributed parameter model for the evaporation system of a supercritical spiral water wall boiler is developed based on a 3-D temperature field. The mathematical method is formulated for predicting the heat flux and the metal-surface temperature. The results show that the influence of the heat flux distribution is more obvious than that of the heat transfer coefficient distribution in the spiral water wall tube, and the peak of the heat transfer coefficient decreases with an increment of supercritical pressure. This distributed parameter model can be used for a 600 MW supercritical-pressure power plant.

Key words: *distributed parameter model, evaporation system, supercritical boiler, spiral water wall*

Introduction

Supercritical, sliding-pressure-operation, once-through boilers have been widely used in thermal generator sets because of their superior properties. The spiral design can be used with fewer tubes to obtain the desired flow per tube by wrapping the tubes around the furnace. The benefit of this arrangement is that the spiral tubes pass the fluid through heat zones to maintain a nearly even fluid temperature at the outlet of the furnace. The wide use of supercritical-pressure water has made heat transfer at supercritical pressures a very important issue.

Research on heat transfer of supercritical fluids has been ongoing since the 1950s. Yamagata and Nishikawa [1] systematically investigated the heat transfer characteristics of supercritical water in tubes and separately proposed some classical correlations to predict the heat transfer coefficient. With the development of supercritical-pressure boilers in China, many investigations on heat transfer of supercritical-pressure water have also been conducted by Yang *et al*. [2]. Because of the complexities of heat transfer at supercritical pressures and the heat-transfer specifics in a combustion chamber of a steam generator, simplifications of the heat flux distribution were usually made for modeling the evaporation system. Li and Huang [3] developed a lumped parameter mathematical model to analyze a helically coiled, once-through steam generator. Pan and Yang [4] calculated the thermal-hydraulic characteristics of a water wall in an ultra-supercritical coal-fired boiler using a distributed parameter model. However, all of these models are based on a reduced one-dimensional heat flux distribution scheme.

Flame image processing techniques have been successfully applied to deal with temperature reconstruction in pc-fired boilers [5]. We have revealed a distributed parameter

* Corresponding author; e-mail: luozixue@mail.hust.edu.cn

model in a subcritical tangential once-through boiler [6], but this model is unsuitable for supercritical spiral-type water-tube boiler owing to the large difference in furnace structure and heat transfer characteristics.

In this paper, a distributed parameter model is proposed for an evaporation system based on 3-D combustion monitoring in a furnace. A mathematical model was formulated for predicting the distributions of the heat flux and the metal-surface temperature to include the non-uniform distribution of the surface heat transfer and the frictional resistance coefficient. The heat transfer characteristics of spiral-wound tubes and a vertical water wall at near-critical and subcritical pressures are illustrated.

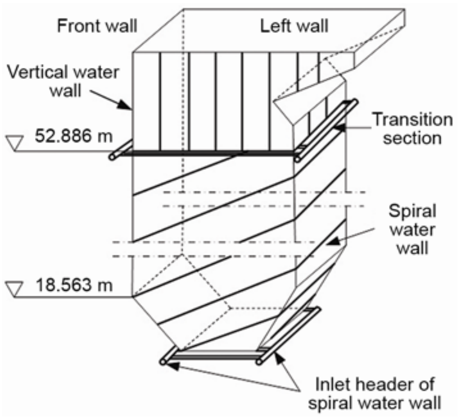

Figure 1. Layout of the evaporation system in a 600 MW, supercritical, once-through boiler

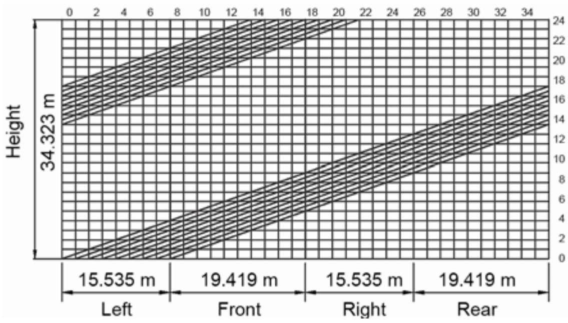

Figure 2. The grids of the unfolded spiral water wall

Mathematical modeling

A 600 MW, supercritical, once-through boiler with spiral-type water tubes in the water wall was chosen as the object of study. The schematic of the boiler and the mesh division are shown in fig. 1 and fig. 2, respectively. The evaporation zone between the ash hopper (18.563 m) and the arch nose (52.886 m) was divided into 25 layers. The horizontal cross-sections of the areas were uniformly divided into 8·10 = 80 elements.

Previous research illustrated the flue gas model and tube wall model in a 300 MW, subcritical, once-through boiler [6]. The 3-D temperature distribution in the furnace can be obtained using the flame image-processing technique in the real-time combustion monitoring system. The 2-D heat flux can be obtained by solving the energy balance equations, which serves as a distributed boundary condition for the dynamic, distributed parameter model of the evaporation system.

The saturated boiling heat transfer coefficient α in a sloped, rifled tube is based on the Lockharte-Martinelli formula [7]:

$$\frac{\alpha}{\alpha_l} = 0.0885\left[\left(\frac{x}{1-x}\right)^{0.9}\left(\frac{\rho_l}{\rho_s}\right)^{0.5}\left(\frac{\mu_s}{\mu_l}\right)^{0.1}\right]^{0.1516}\left(\frac{p}{22.115}\right)^{-5.2231}\left(\frac{G}{2000}\right)^{-0.1664} \tag{1}$$

The critical quality x_{cr} (which characterizes the heat transfer deterioration of the second kind) is given by [2]. According to the Slaughterback empirical relation [8], the formula for the post-dryout-region heat transfer coefficient in a sloped, rifled tube is given by:

$$\alpha = 0.014132\frac{\lambda}{d}\{\mathrm{Re}_s[x+\frac{\rho_s}{\rho_l}(1-x)]\cdot 10^{-6}\}^{1.2531}\,\mathrm{Pr}_b^{0.8548}\left(\frac{\lambda_s}{\lambda_{cr}}\right)^{-0.3833}\left(\frac{p}{22.115}\right)^{-1.3041} \quad (2)$$

The formula for the frictional resistance coefficient can be given by [2].

In the supercritical pressure range, the heat transfer characteristics of water in tube strongly depend on the variations in the physical properties. As shown in fig. 3, the specific heat capacity has a local maximum at the pseudo-critical temperature. The thermal conductivity as well as the density and the dynamic viscosity decrease dramatically within a very narrow temperature range near the pseudo-critical point. Figure 4 shows that the changes in the thermo-physical properties become less pronounced in the heat transfer behavior at higher supercritical pressures.

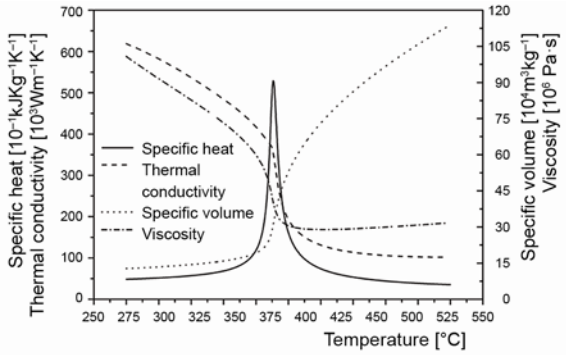

Figure 3. Thermal-physical properties of water versus temperature at 26 MPa

The heat transfer coefficient at supercritical pressures is expressed by [9]:

$$\alpha = 0.0068\frac{\lambda}{d}\mathrm{Re}_b^{0.9}\,\mathrm{Pr}_b^{0.63}\left(\frac{\rho_w}{\rho_b}\right)^{0.17}\left(\frac{\lambda_w}{\lambda_b}\right)^{0.29} \quad (3)$$

The parameters in these calculations can be got by calling the related functions which are based on IAPWS-IF97.

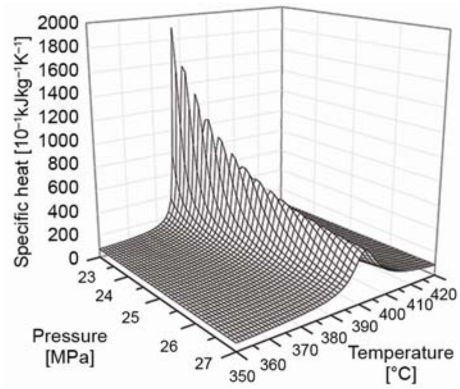

Figure 4. The effect of pressure on the specific heat of water at supercritical pressures

Results and discussions

The test cases are listed in tab. 1. A monitoring instrument was installed to capture the temperature at a height of 52.886 m. The measured wall temperatures and the calculated values are shown in fig. 5. The mass velocity can be obtained after summation of all the units in a tube:

$$\sum_{i=1}^{25}\xi_i\frac{(\rho w)^2}{2\rho_i} = \Delta p - \sum_{i=1}^{25}\rho_i H_i \mathrm{g}\sin\theta \quad \theta = 19.471° \quad (4)$$

Table 1. Operational data in the simulation

Case	Load [MW]	Steam pressure [MPa]	Feedwater quantity [th^{-1}]	Feedwater temperature [°C]
1	300	16.03	914.20	235.00
2	480	23.01	1369.0	255.47
3	600	28.68	1710.0	269.70

As shown in fig. 5, the maximum relative difference between the simulation results and the measurements is 0.6%, the maximum temperature difference is 4 °C and the mass ve-

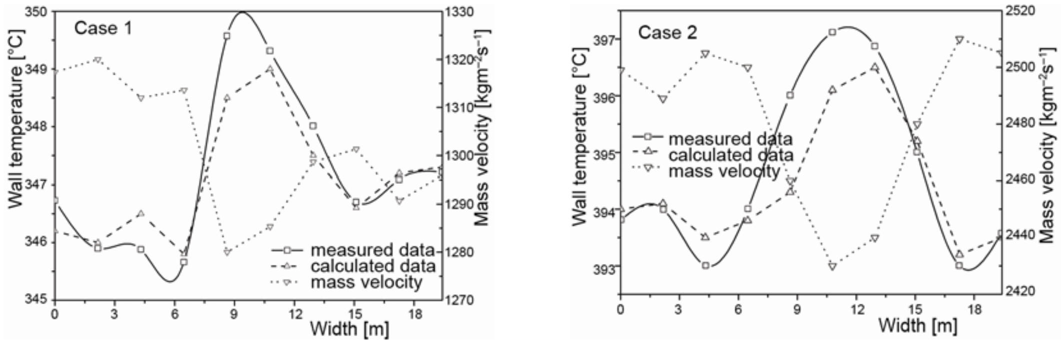

Figure 5. Comparison of temperature and mass flow distributions in front wall

locity difference is 3.2%. The results show the mathematical model for predicting the metal temperatures of tubes are fit for *in-situ* operation.

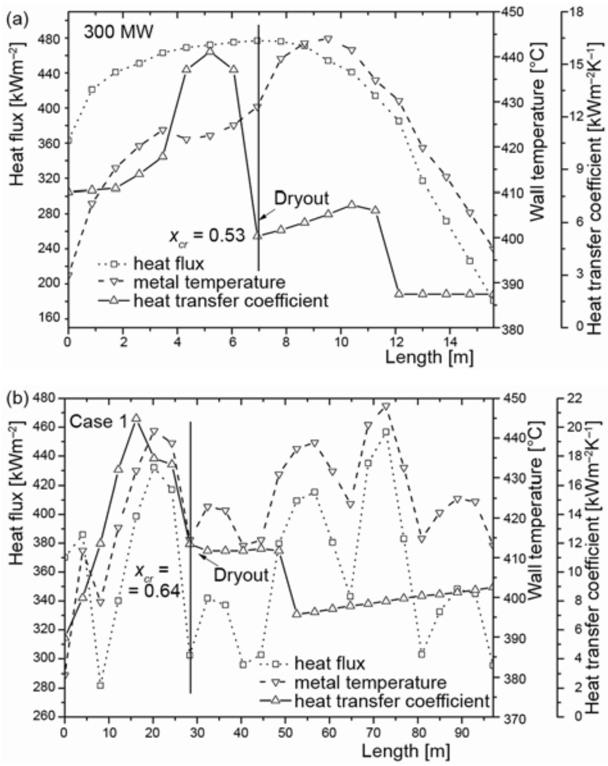

Figure 6. Comparison of heat transfer characteristic in a single tube on different types of water walls at a subcritical pressure: (a) vertical water wall, (b) spiral water wall

Figure 6 gives a comparison of the wall temperature and heat transfer coefficient distributions for the vertical water wall and the spiral water wall at a subcritical pressure. As shown in fig. 6(b), a single tube is able to by-pass the different furnace walls, and heat absorption is homogenous with the rising spiral along the furnace perimeter, so the heat difference is effectively eliminated. As the steam quality reaches a certain critical value, which is 0.53 in fig. 6(a) and 0.64 in fig. 6(b), the water state has changed from saturated boiling to post-dryout. However, the corresponding heat flux is maximum in the vertical water wall tube, whereas the heat flux is at the local minimum in case of the spiral water wall tube. Therefore, the wall temperature increases in the vertical tube, but this can be avoided in the spiral tube.

Whereas the wall temperature is influenced by the heat flux and the heat transfer coefficient distribution, the influence of the heat flux is larger than that of the heat transfer coefficient in the spiral water wall tube. There are two reasons: one is that the fluid temperature is at the saturated temperature all the time after vaporizing, the other is that the heat flux presents a wave distribution in the spiral water wall tube. Therefore, assuming a non-uniform heat flux distribution strongly affects the accuracy of the model.

Figure 7 illustrates a comparison of the wall temperature and heat transfer coefficient distributions at a near-critical pressure and those at a supercritical pressure in the spiral water wall. As shown in fig. 7, the heat transfer coefficient rises to the maximum of 36 kW/m²K when H_{pc} = 2092.6 kJ/kg in case 2 and it rises to the maximum of 21 kW/m²K when H_{pc} = 2106.1 kJ/kg in case 3. So, the maximum heat transfer coefficients are located in the pseudo-critical enthalpy region. This means that the heat transfer of supercritical water in the pseudo-critical enthalpy range is effectively enhanced.

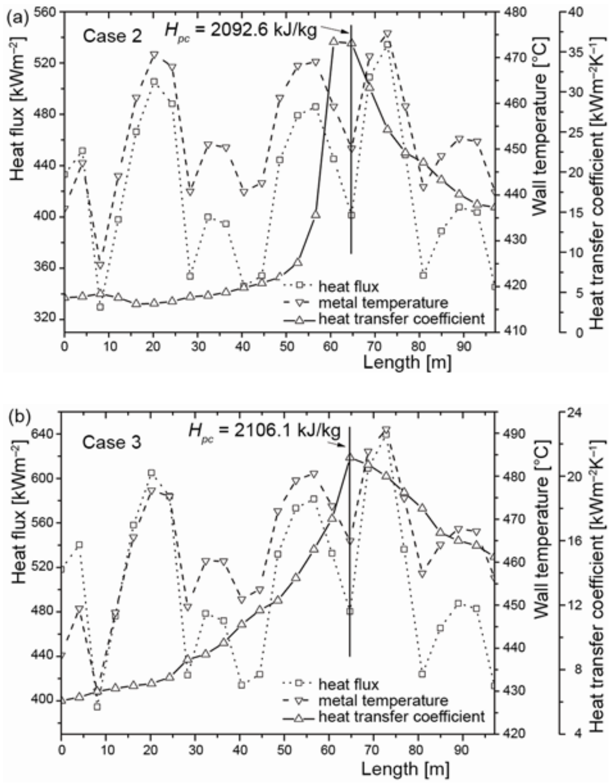

Figure 7. Comparison of heat transfer characteristics in a single tube at different pressures in a spiral water wall: *(a) near-critical pressure, (b) supercritical pressure*

Figure 7 shows that the peak of the heat transfer coefficient in case 2 is 15 kW/m²K larger than in case 3. It means that the peak of the heat transfer coefficient decreases and the bulk fluid enthalpy corresponding to the peak of the heat transfer coefficient increases with an increase in supercritical pressure. With increasing heat flux, more fluid is heated to a temperature above the pseudo-critical temperature point. In other words, the portion of the fluid that is responsible for the enhancement of heat transfer is suppressed: as observed in case 3, the heat transfer coefficients decrease so the tube achieves an optimum heat transfer effect in case 2.

Conclusions

A distributed parameter model for an evaporation system in a supercritical, spiral water wall boiler was established. A method for predicting the distributions of the heat flux and the metal-surface temperature in the evaporation system was proposed based on 3-D temperature fields. The simulation results show that the influence of the heat flux distribution is larger than that of the heat transfer coefficient distribution in the spiral water wall tube. The maximum heat transfer coefficients are located in the pseudo-critical enthalpy region and the peak of the heat transfer coefficient decreases by 15 kW/m²K with an increment of supercritical pressure. The water wall can produce a more desirable heat transfer effect according to this distributed parameter model.

Nomenclature

c_p – specific heat capacity, [Jkg^{-1}K^{-1}]
d – diameter, [m]
G – mass velocity, [kgm^{-2}s^{-1}]
g – acceleration of gravity, [ms^{-2}]

H – height, [m]
p – pressure, [Pa]
Pr – Prandtl number (= $\mu c_p/\lambda$), [–]
Re – Reynolds number (= $\rho wd/\mu$), [–]
w – velocity, [ms^{-1}]
x – steam quality, [–]

Greek symbols

α – heat transfer coefficient, [$Wm^{-2}K^{-1}$]
Δ – difference in any quantity
λ – thermal conductivity, [$Wm^{-1}K^{-1}$]
μ – dynamic viscosity, [$Nm^{-1}s^{-1}$]
ξ – resistance coefficient
ρ – density, [kgm^{-3}]

Subscripts

b – bulk
cr – critical point
i – number of element
l – liquid
s – steam
w – water wall

Acknowledgments

This work is sponsored by the National Natural Science Foundation of China (Contract Nos.: 51076049, 51025622 and 50721005).

References

[1] Yamagata, K., Nishikawa, K., Forced Convection Heat Transfer to Supercritical Water Flowing in Tubes, *International Journal of Heat and Mass Transfer*, *15* (1972), 12, pp. 2575-2593
[2] Yang, D., Pan, J., Experimental Investigation on Heat Transfer and Frictional Characteristics of Vertical upward Rifled Tube in Supercritical CFB Boiler, *Experimental Thermal and Fluid Science*, *35* (2011), 2, pp. 291-300
[3] Li, H., Huang, X., A Lumped Parameter Dynamic Model of the Helical Coiled Once-through Steam Generator with Movable Boundaries, *Nuclear Engineering and Design*, *238* (2008), 7, pp. 1657-1663
[4] Pan J., Yang D., Mathematical Modeling and Thermal-Hydraulic Analysis of Vertical Water Wall in an Ultra Supercritical Boiler, *Applied Thermal Engineering*, *29* (2009), 11-12, pp. 2500-2507
[5] Zhou, H. C., *et al.,* Experimental Investigations on Visualization of Three-Dimensional Temperature Distributions in a Large-Scale Pulverized-Coal-Fired Boiler Furnace, *Proceedings*, 30th International Symposium on Combustion, Chicago, USA, 2005, Vol. 30, pp. 1699-1706
[6] Zheng, S., Luo, Z., Distributed Parameters Modeling for Evaporation System in a Once-Through Coal-Fired Twin-Furnace Boiler, *International Journal of Thermal Sciences, 50* (2011), 12, pp. 2496-2505
[7] Chen, J. C., Correlation for Boiling Heat Transfer to Saturated Fluids in Convective Flow, *Industrial and Engineering Chemistry Research*, *5* (1966), 3, pp. 322-329
[8] Polyakov, A. F., Heat Transfer under Supercritical Pressures, *Advanced in Heat Transfer 21* (1991), 1, pp. 1-51
[9] Zhu, X., Bi, Q. C., An Investigation on Heat Transfer Characteristics of Different Pressure Steam-Water in Vertical Upward Tube, *Nuclear Engineering and Design*, *239* (2009), 2, pp. 381-388

Paper submitted: January 18, 2013
Paper revised: April 26, 2013
Paper accepted: June 2, 2013